Chinese Journal of Aeronautics, (2015), 28(5): 1485–1493

Chinese Society of Aeronautics and Astronautics
& Beihang University

Chinese Journal of Aeronautics

cja@buaa.edu.cn
www.sciencedirect.com

Difference beam aided target detection in monopulse radar

Cai Fei *, **Fan Hongqi, Song Zhiyong, Fu Qiang**

ATR Key Laboratory, National University of Defense Technology, Changsha 410073, China

Received 18 December 2014; revised 25 May 2015; accepted 3 August 2015
Available online 28 August 2015

KEYWORDS

Detection;
Difference beam;
Monopulse radar;
Sum beam;
Generalized likelihood ratio test

Abstract The classical detection step in a monopulse radar system is based on the sum beam only, the performance of which is not optimal when target is not at the beam center. Target detection aided by the difference beam can improve the performance at this case. However, the existing difference beam aided target detectors have the problem of performance deterioration at the beam center, which has limited their application in real systems. To solve this problem, two detectors are proposed in this paper. Assuming the monopulse ratio is known, a generalized likelihood ratio test (GLRT) detector is derived, which can be used when targeting information on target direction is available. A practical dual-stage detector is proposed for the case that the monopulse ratio is unknown. Simulation results show that performances of the proposed detectors are superior to that of the classical detector.

1. Introduction

Monopulse is a widely used technique to provide accurate angle measurements in the tracking radar.[1] A monopulse system for estimating one angle typically consists of two identical antennas, either separated by some distance (phase monopulse) or at the same phase center but with a squint angle (amplitude monopulse), whose outputs are summed up to produce a sum beam Σ and are subtracted to yield the difference beam Δ. The angular information θ is contained in the monopulse ratio $\gamma = \Delta(\theta)/\Sigma(\theta)$ provided that the function $\theta \rightarrow \gamma(\theta)$ is invertible.[2–4]

The open literature[5–8] has revealed a separate analysis of detection and estimation. The detection step has been performed with the sum beam only, while the difference beam is used only for angle estimation. In Refs.[9–12], angle estimation conditioned on the detection has been studied, however, the detections in them are performed with the sum beam only, too. The classical sum beam detector is optimal provided the boresight is close to the true target direction, since amplitude of the difference beam is approximately zero there. However, amplitude of the difference beam is comparable to that of the sum beam near the sum beam half-power point. Thus it is possible to utilize the difference beam to improve the detection performance.

Armstrong and Griffiths[13] firstly proposed the idea of using difference beam at the detection step. Two realizations of this idea were presented. One of them is to use different linear

* Corresponding author. Tel.: +86 731 84576401 0.
E-mail address: caifei.nudt@qq.com (F. Cai).

Peer review under responsibility of Editorial Committee of CJA.

http://dx.doi.org/10.1016/j.cja.2015.08.007

combinations of the sum and difference beams as the test statistics. It was shown that certain combinations can give a detection gain relative to the sum beam only detection. The other one is based on the complex indicated angle. Constant false-alarm rate (CFAR) performance has been achieved without using adjacent cells as references. However, the CFAR loss of this method is comparatively high. Chaumette et al.[14,15] applied optimal detection theory to this problem. They treated the difference aided detection as a composite hypothesis testing problem and obtained the generalized likelihood ratio test (GLRT) under some approximation, which is referred to as the Power-Mosca detector-estimator solution. The Power-Mosca detector is similar to the linear combination method in Ref.[13] It combines the sum and difference beam with equal weights irrespective of the deviation angle. As a result, the performance is improved at the beam edge but deteriorated at the beam center.

In this paper, we use the monopulse ratio as the weight of the difference beam and take weighted sum of the sum and difference beams as the test statistic to get performance improved at the beam edge while keeping the performance at the beam center. For the cases that the monopulse ratio is known or unknown, two practical difference beam aided detectors are proposed. The performances of the two detectors are studied via Monte Carlo simulations.

2. Signal model

Firstly we take the phase monopulse as an example to show the angle estimation process in monopulse systems. In the case of phase monopulse with two antennas separated by a distance L as shown in Fig. 1, the phase difference φ between the two antennas is

$$\varphi = \frac{2\pi}{\lambda} L \sin\theta \tag{1}$$

where λ is the wavelength and θ the deviation angle from boresight. Let E_1 and E_2 denote the two monopulse antenna outputs. The sum and difference beam have the form (ignoring receiver noise):

$$\begin{cases} \Sigma = E_1 + E_2 = 2E_1 \cos(\varphi/2)\exp(\mathrm{j}\cdot\varphi/2) \\ \Delta = E_2 - E_1 = 2\mathrm{j}E_1 \sin(\varphi/2)\exp(\mathrm{j}\cdot\varphi/2) \end{cases} \tag{2}$$

Therefore the monopulse ratio γ takes the form

$$\gamma = \Delta/\Sigma = \mathrm{j}\cdot\tan(\varphi/2) = \mathrm{j}\cdot\tan\left(\frac{\pi}{\lambda}L\sin\theta\right) \tag{3}$$

which is a fairly linear function in the neighborhood of the look direction (i.e., θ is small). The angle θ can then be calculated using the monopulse ratio γ. Typical sum and difference beam patterns are shown in Fig. 2. Readers could refer to Ref.[2] for detail.

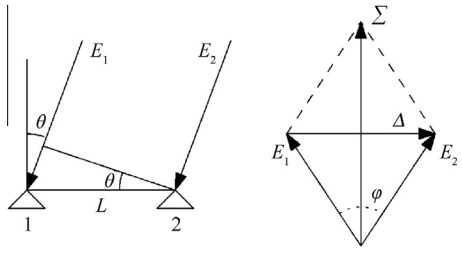

Fig. 1 Pictorial description of phase monopulse.

In practical monopulse systems, the receiver noise is present, and the received signal can be modeled as two parallel sequences $\{x_i\}$ (sum beam), $\{y_i\}$ (difference beam) of complex-valued voltage samples representing amplitude and phase of the N pulse returns from a target.[8] The radar target is considered to be a point target whose return signal is assumed to be non-fluctuating from pulse to pulse. Jamming is assumed to be absent so that the target signal competes only against receiver thermal noise. To unify the phase and amplitude monopulses, the imaginary unit j in γ (which exists only in phase monopulse) is dismissed and γ is real. The signal model under the null hypothesis (noise only) H_0 and the alternate hypothesis (signal plus noise) H_1 is

$$\begin{aligned} H_0 &: \boldsymbol{x} = \boldsymbol{u},\ \boldsymbol{y} = \boldsymbol{v} \\ H_1 &: \boldsymbol{x} = \boldsymbol{a} + \boldsymbol{u},\ \boldsymbol{y} = \gamma\boldsymbol{a} + \boldsymbol{v} \end{aligned} \tag{4}$$

where $\boldsymbol{x}\triangleq\{x_i\}$, $\boldsymbol{y}\triangleq\{y_i\}$, $\boldsymbol{a}\triangleq\{a_i\}$, $\boldsymbol{u}\triangleq\{u_i\}$, $\boldsymbol{v}\triangleq\{v_i\}$ are $N\times 1$ column vectors and γ is the monopulse ratio, which is considered constant over the N pulses (Because the range between target and radar is long, the effect of target's movement within N pulses on its DOA can be neglected); $a_i\triangleq a_{\mathrm{I}i} + \mathrm{j}a_{\mathrm{Q}i}$ is the complex amplitude of the i th pulse return from direction γ, which is unknown; $\{u_i\}$ and $\{v_i\}$ are the stationary complex Gaussian noise processes with zero means and variance σ^2 associated with observables $\{x_i\}$ and $\{y_i\}$, respectively (The unbalance of the sum and difference channels' noise levels can be adjusted at the initialization stage of the monopulse radar); Independence between and among the Gaussian processes $\{u_i\}$, $\{v_i\}$ is assumed.

Under this signal model, the classical sum beam detector can be formulated as

$$||\boldsymbol{x}||^2 > T \tag{5}$$

where $||\boldsymbol{x}||^2\triangleq\sum_{i=1}^{N}|x_i|^2$ and T is the detection threshold. The sum beam detector Eq. (5) is referred to as the Classical detector in the remainder of this paper. The Power-Mosca detector proposed in Ref.[15] has the form

$$||\boldsymbol{x}||^2 + ||\boldsymbol{y}||^2 > T \tag{6}$$

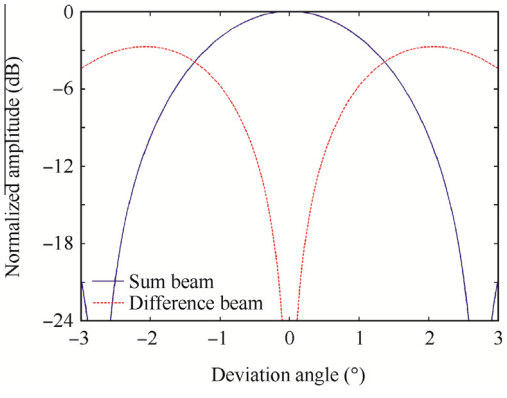

Fig. 2 Typical sum and difference beam patterns of monopulse.

3. GLRT detector: γ is known

Both Ref.[13] and Ref.[15] have only considered the case that γ is unknown. In fact, in tracking radar application, there may be targeting data from other sensors on the target's angular information. Difference beam aided detection in this case is meaningful since it can make full use of the priori information. So firstly we consider the difference beam aided detection in the case that γ is known, which has never been considered in the monopulse paradigm to the best of our knowledge.

From Eq. (4) we can get that

$$p(\boldsymbol{x},\ \boldsymbol{y}|H_0)=\frac{1}{(\pi\sigma^2)^{2N}}\exp\left\{-\frac{1}{\sigma^2}[\boldsymbol{x}^{\mathrm{H}}\boldsymbol{x}+\boldsymbol{y}^{\mathrm{H}}\boldsymbol{y}]\right\} \tag{7}$$

and

$$\begin{aligned}p(\boldsymbol{x},\ \boldsymbol{y}|\boldsymbol{a},\ H_1)&=\frac{1}{(\pi\sigma^2)^{2N}}\\&\times\exp\left\{-\frac{1}{\sigma^2}[(\boldsymbol{x}-\boldsymbol{a})^{\mathrm{H}}(\boldsymbol{x}-\boldsymbol{a})+(\boldsymbol{y}-\gamma\boldsymbol{a})^{\mathrm{H}}(\boldsymbol{y}-\gamma\boldsymbol{a})]\right\}\end{aligned} \tag{8}$$

The optimal detection rules are not realizable since there is a unknown parameter $\boldsymbol{a}$. A common approach for designing realizable tests in this case is to replace the unknown parameters with estimates, and then the detection problem becomes a composite hypothesis testing problem.[16] The GLRT for deciding whether to accept H_0 or to accept H_1 is given by

$$L_{\mathrm{G}}(\boldsymbol{x},\boldsymbol{y})=\frac{p(\boldsymbol{x},\boldsymbol{y}|\hat{\boldsymbol{a}},H_1)}{p(\boldsymbol{x},\boldsymbol{y}|H_0)}>T \tag{9}$$

where $\hat{\boldsymbol{a}}$ stands for the maximum likelihood estimation (MLE) of the unknown parameter $\boldsymbol{a}$ under hypothesis H_1.

The MLE of $\boldsymbol{a}$ can be calculated by

$$\frac{\partial\ln p(\boldsymbol{x},\boldsymbol{y}|\boldsymbol{a},H_1)}{\partial\boldsymbol{a}}=0 \tag{10}$$

After a few lines of algebra we can get

$$\hat{\boldsymbol{a}}=\frac{\boldsymbol{x}+\gamma\boldsymbol{y}}{1+\gamma^2} \tag{11}$$

Substituting Eq. (11) into Eq. (9), we get the GLRT detector

$$\mathrm{GLRT}:\ ||\boldsymbol{x}+\gamma\boldsymbol{y}||^2>T \tag{12}$$

Probability of false alarm P_{FA} and probability of detection P_{D} of the GLRT detector can be calculated by

$$\begin{aligned}P_{\mathrm{FA}}&=\int_{\frac{2T}{\sigma^2(1+\gamma^2)}}^{\infty}\frac{t^{N-1}\exp(-t/2)}{2^N\Gamma(N)}dt\\P_{\mathrm{D}}&=\int_{\frac{2T}{\sigma^2(1+\gamma^2)}}^{\infty}\frac{1}{2}(t/\eta)^{(N-1)/2}\exp[-(t+\eta)/2]I_{N-1}(\sqrt{\eta t})\mathrm{d}t\end{aligned} \tag{13}$$

where $\Gamma(u)$ is the Gamma function, $I_{\mathrm{r}}(u)$ is the modified Bessel function of the first kind, and the non-centrality parameter η is

$$\eta=\frac{2(1+\gamma^2)||\boldsymbol{a}||^2}{\sigma^2} \tag{14}$$

The proofs of Eq. (13) are omitted here and readers can refer to Ref.[16] for similar results.

Eq. (13) can be further simplified to the following expression[16]:

$$P_{\mathrm{FA}}=\exp\left(-\frac{T}{\sigma^2(1+\gamma^2)}\right)\sum_{n=0}^{N-1}\frac{1}{n!}\left(\frac{T}{\sigma^2(1+\gamma^2)}\right)^n \tag{15}$$

4. Dual-stage detector: γ is unknown

Now we consider a more general case that γ is unknown. From Eqs. (6) and (12) we can deduce that to avoid performance loss in the beam center, the difference beam should be weighted by the monopulse ratio γ. As the deviation angle is unknown in this case, a straightforward way is to estimate the γ firstly and then use the estimate $\hat{\gamma}$ as the weight of the difference beam. However, if we estimate γ directly using the input signal, $\hat{\gamma}$ might be unreasonably high since the sum beam contains zero mean noise only under H_0 hypothesis. Taking this into account, a dual-stage detection structure is proposed as shown in Fig. 3. The primary stage is a classical detector with a low threshold T_1, which uses sum beam only. If the primary stage detection is passed, $\hat{\gamma}$ is calculated, and the weighted sum of the sum and difference beam using $\hat{\gamma}$ is the test statistic of the secondary stage detection.

There are two more questions to be answered for the structure selected: one of them is to choose the calculation method of $\hat{\gamma}$ using the N pulses; the other is to choose suitable primary threshold, T_1. The secondary threshold T_2 can be uniquely determined once T_1 is given.

4.1. Calculation of $\hat{\gamma}$

To select the method of calculating $\hat{\gamma}$, the two hypothesis H_0 and H_1 should be considered separately: under H_1, the calculation of $\hat{\gamma}$ is to estimate γ, and the accuracy of the estimation is what we seek under H_0, γ does not exist physically, thus we expect $\hat{\gamma}$ to be as small as possible to decrease the false alarms.

The most simple method of monopulse ratio estimation under this context is to average the N estimated angles[17], the expression of which is

$$\hat{\gamma}_{\mathrm{Mean}}=\frac{1}{N}\sum_{i=1}^{N}\mathrm{Re}\left(\frac{y_i}{x_i}\right) \tag{16}$$

Another estimator is the maximum likelihood (ML) estimator derived by Mosca[8], which has since become the practical monopulse ratio estimator. The ML estimator has the following expression:

$$\hat{\gamma}_{\mathrm{ML}}=\frac{\mathrm{Re}(\boldsymbol{x}^{\mathrm{H}}\boldsymbol{y})}{||\boldsymbol{x}||^2} \tag{17}$$

We choose the two estimators as the potential calculation methods of $\hat{\gamma}$ and select one of them by comparing their performances under H_1 and H_0, respectively.

For $N=1$, from Eqs. (16) and (17) we can get that the two methods are the same. For other values of N, it is not the case at all. It is known that estimation performance of Eq. (17) is better than that of Eq. (16) under H_1. Thus we only compare their behavior under H_0 in this study. We use the

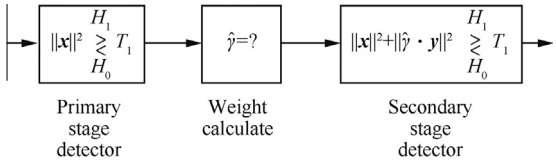

Fig. 3 Structure of dual-stage detector.

Kaplan–Meier estimate of the cumulative distribution function (CDF) as the measure, which is also known as the empirical CDF (ECDF). Fig. 4 shows the ECDF curves of the two methods under H_0, in which results for $N = 2, 3, \ldots, 8$ are presented. We see that each curve of the ML method is above that of the Mean method, which means that the $\hat{\gamma}$ calculated by the ML method is smaller than that of the Mean method for the adopted N. Combining the two factors above, the ML estimator can be selected as the method to calculate the $\hat{\gamma}$.

4.2. Choice of primary thresholds T_1

We know that in the dual-stage detection structure, we can keep final probability of false alarm P_{FA} fixed at a constant value by raising one threshold and lowering the other. Because the calculation of $\hat{\gamma}$ is conditioned on the primary detection, T_1 should be as high as possible to make $\hat{\gamma}$ accurate under H_1[18] and small under H_0. But if T_1 is too high, the signal at the edge of the beam cannot pass the primary detection because its power is lower than that at the beam center, which will limit the P_D at the beam edge. Thus, a compromise between them should be made.

To see how T_1 affects P_D at the beam center and at the beam edge, we keep $P_{FA} = 10^{-4}$ constant and vary the primary probability of false alarm P_{FA1} from 10^{-3} to 0.5. The corresponding P_D at beam angles 0° and 1.2° is shown in Fig. 5. We see that at the beam center (0°), P_D is a monotonic decreasing function of P_{FA1}, and when P_{FA1} is less than 0.06 the decrement is small. We can also see that at the beam edge (1.2°), P_D is a parabolic curve of P_{FA1} and reaches the maximum approximately at $P_{FA1} = 0.05$. Thus considering the two aspects and recalling our aim to get performance improved at the beam edge while keeping performance at the beam center, it is justifiable to set $P_{FA1} = 0.05$ in this case. The primary threshold T_1 can then be computed using the inverse chi-square CDF with $2N$ degrees of freedom for the corresponding probabilities in P_{FA1}. That is,

$$T_1 = F^{-1}(P_{FA1}|N) = \{T_1 : F(T_1|N) = P_{FA1}\} \tag{18}$$

where

$$P_{FA1} = F(T_1|N) = \int_{2T_1/\sigma^2}^{\infty} \frac{t^{N-1}e^{-t/2}}{2^N \Gamma(N)} dt \tag{19}$$

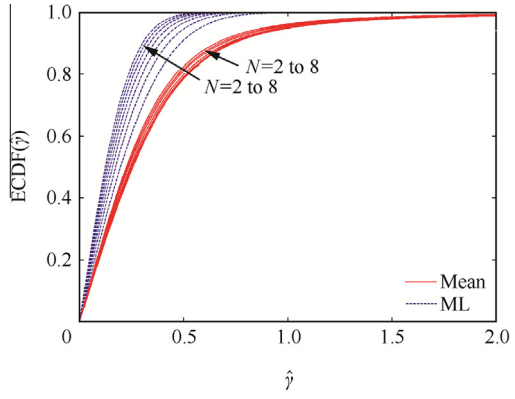

Fig. 4 ECDF curves of ML and mean monopulse estimation method under H_0.

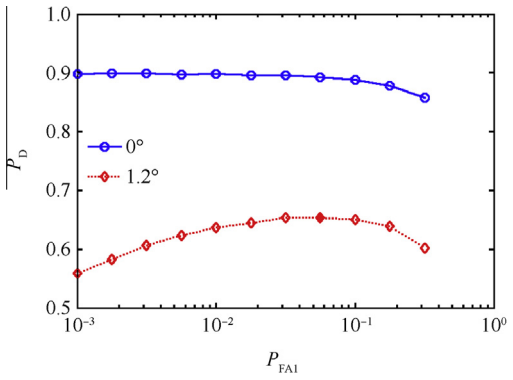

Fig. 5 P_D of angle points 0° and 1.2° as functions of P_{FA1}, 5 pulses.

Note that for a different setting of radar parameters (e.g., a different pulse number N), the result might be different and it should be determined using the given radar parameters.

Secondary probability of false alarm P_{FA2} can be calculated by $P_{FA2} = P_{FA}/P_{FA1}$ once P_{FA1} is determined. Because the secondary stage detection is conditioned on the primary detection, the secondary threshold T_2 is hard to obtain by theoretical calculation. A Monte Carlo method is used as follows. Firstly acquire a large number of samples randomly under H_0 and do first stage detection on them. Then calculate the test statistics of the secondary detection on those samples that have passed T_1. After that, calculate the ECDF using the test statistics. Finally, get T_2 by P_{FA2} and the ECDF. This procedure is summarized in Table 1, where N_r is the number of Monte Carlo runs used and $CN(0, \sigma^2)$ is the complex Gaussian distribution with mean 0 and variance σ^2.

5. Numerical results

In this section we use a simulated phase monopulse radar to evaluate the performances of the two detectors. The sum and difference beam patterns of a phase monopulse radar can be approximated by the following expressions[18,19]:

$$\begin{aligned} \Sigma(\theta) &= \cos(\theta)^{\frac{\lg(1/\sqrt{2})}{\lg(\cos(\beta/2))}} \cos\left(\frac{\pi L}{\lambda}\sin(\theta)\right) \\ \Delta(\theta) &= \cos(\theta)^{\frac{\lg(1/\sqrt{2})}{\lg(\cos(\beta/2))}} \sin\left(\frac{\pi L}{\lambda}\sin(\theta)\right) \end{aligned} \tag{20}$$

Table 1 Procedure for getting secondary threshold.

Steps of algorithm
set $j = 0$
for $k = 1 : N_r$ do
draw $u_i, v_i \sim CN(0, \sigma^2), i = 1, 2, \ldots, N$
$\boldsymbol{x} = [u_i]_{i=1}^N, \boldsymbol{y} = [v_i]_{i=1}^N$
if $\|\|\boldsymbol{x}^2\|\| > T_1$ then
$j = j + 1, \hat{\gamma} = \mathrm{Re}(\boldsymbol{x}^H\boldsymbol{y})/\|\|\boldsymbol{x}^2\|\|$
end
end
$[\{p_i\}_{i=1}^j, \{s_i\}_{i=1}^j] = \mathrm{ECDF}(\{t_i\}_{i=1}^j)$
$\hat{i} = \arg\min_i(\|1 - P_{FA2} - p_i\|)$
$T_2 = s_{\hat{i}}$

where β is the half-power beamwidth of each antenna, L the distance between the two antennas, and λ the wavelength. These expressions are used for all the numerical analysis throughout this paper, with $\beta = 5°$; $L = 7.62$ cm and $\lambda = 8$ mm, which yield the sum and difference beam patterns as shown in Fig. 2.

5.1. Performance of GLRT detector

Performance of the GLRT detector can be calculated directly from Eq. (13). Its performance as well as that of the Classical detector are presented in Fig. 6, where the sum beam signal-to-noise ratio (SNR) is adjusted to provide $P_D = 0.9$ at the beam center for the Classical detector under the constraint $P_{FA} = 10^{-4}$. We can see that if γ is perfectly known, performances at the beam center are the best for both the two detectors, where $\gamma = 0$ and the GLRT detector is equivalent to the Classical detector. So it can be concluded that for the sake of the detection performance, the boresight should be placed to the true target direction (if possible) even if the difference beam aided detection is applied. If two or more targets exist within the beam and their deviation angles are different, then not all of them can be placed at the beam center, and in this case the GLRT detector can be used to improve the detection performance of those not at the beam center.

In practice, the targeting information of the deviation angle θ may be inaccurate. In this case the targeting information can generally be described by some probability distribution such as the normal distribution. To see the performance of the GLRT detector in this case, we assume that the targeting information has a normal distribution $\theta \sim N(\mu_\theta, \sigma_\theta^2)$, with the mean μ_θ at discrete angle points $0°, 0.3°, \ldots, 2.4°$ and the stand deviation taking values of $\sigma_\theta = 0.5°, 1.0°, 1.5°, 2°$, respectively. The monopulse ratio used by the GLRT detector is set as $\gamma = \Delta(\mu_\theta)/\Sigma(\mu_\theta)$. The results of Monte-Carlo simulation are also shown in Fig. 6. We see that as the deviation of the targeting information increases, deterioration of the P_D performance increases too. When the deviation of the targeting information is too high, the P_D performance is unacceptable and the GLRT detector is not applicable. In this case we can ignore the targeting information and adopt the dual-stage detector.

5.2. Performance of dual-stage detector

In this section, performance of the developed dual-stage detector is studied through simulation. For comparison, performances of the Classical detector and the Power-Mosca detector are also presented. For all these studies, $P_{FA} = 10^{-4}$, and all P_{FA} and P_D indices are evaluated on 10^8 and 10^5 Monte-Carlo trials, respectively.

Fig. 7 presents the P_D performances at different deviation angles, where the SNR is adapted to provide $P_D = 0.9$ for the Classical detector at the beam center. We see that except for a small region near the beam center, the dual-stage detector

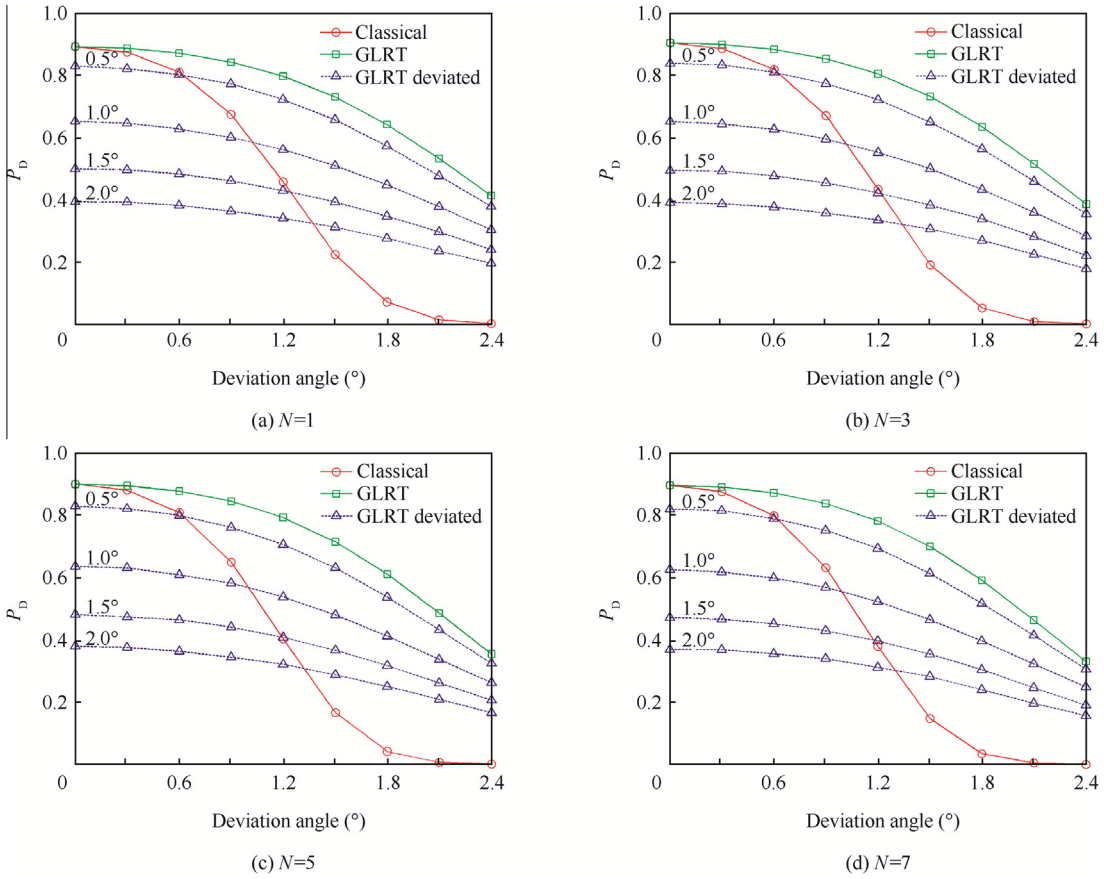

Fig. 6 P_D of classical detector, GLRT detector and GLRT detector when targeting information is inaccurate.

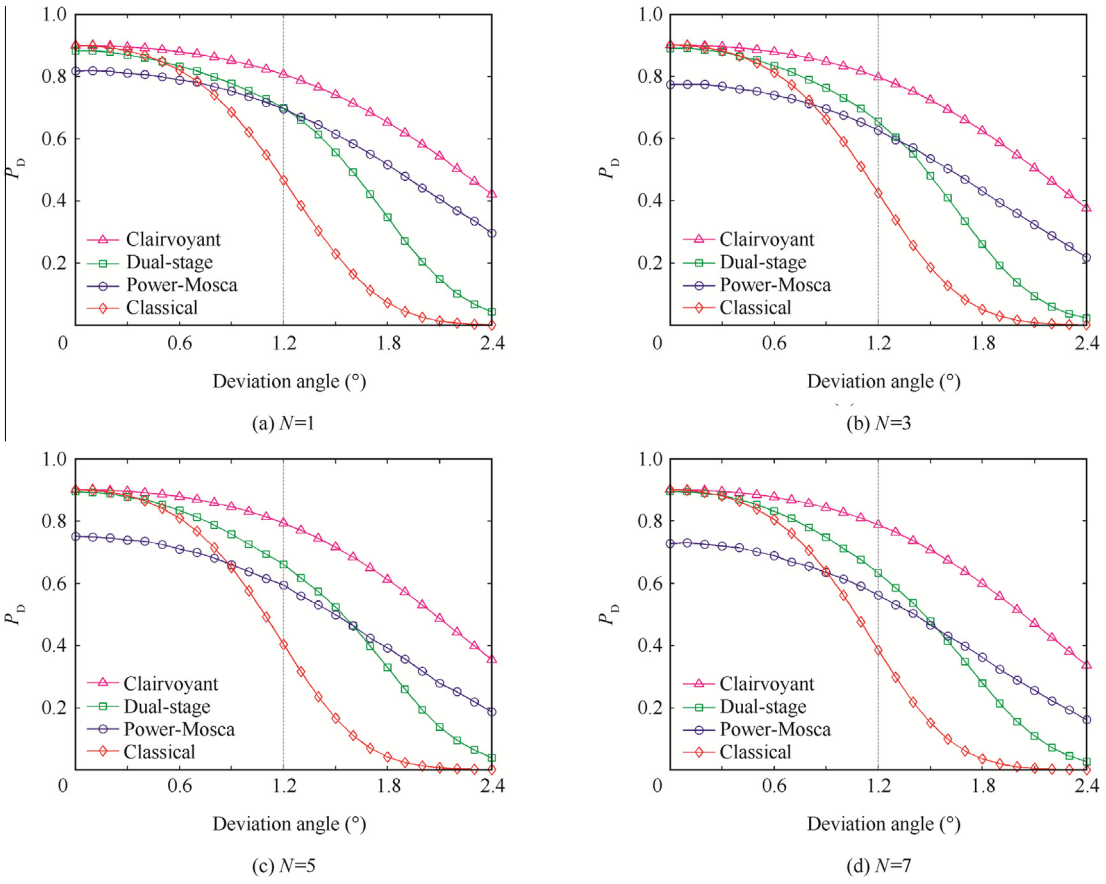

Fig. 7 P_D for dual-stage detector at different deviation angles (the gray dashed lines indicate position of sum beam half-power point).

is superior to the Classical detector. The performance improvement is significant when the deviation angle is near the half-power point. The performance loss of the Power-Mosca detector at the beam center is severe, and as N increases, the performance loss increases too, while that of the dual-stage detector is kept very small. Additionally, we see that the dual-stage detector outperforms the Power-Mosca detector within the sum beamwidth in all the four cases. Comparing the curves of the proposed detector and the Classical detector, we see that the proposed detector has increased the half-power beamwidth equivalently in the detection performance sense. A detector that assumes perfect knowledge of an unknown parameter to design the NP detector is referred to as a clairvoyant detector, the performance of which is used as an upper bound.[16] In Section 3, we get the GLRT detector through assuming the monopulse ratio γ is known. The GLRT detector can be taken as the clairvoyant detector for the case that γ is unknown. Hence performance of the GLRT detector is also presented in Fig. 7 to show the upper bound of difference beam-aided target detection.

The angle estimation accuracy is a crucial index for a monopulse radar. Although the dual-stage detector and the Power-Mosca solution use the same monopulse estimation method that is derived by Mosca, their detector structures are different, which select the subset of observations participating in the estimation and result in different estimation performances.[20] Thus, the conditional root mean squared error (RMSE) of them are evaluated using Monte-Carlo simulation. For comparison, the angle estimation conditioned by the Classical detector is also evaluated. The SNR setup is the same as that of Fig. 7. The performance comparison as shown in Fig. 8 reveals that the dual-stage detector provides a comparatively good angle estimation performance in all the four cases.

Fig. 9 shows the comparison of the overall detection performances between the three detectors under the assumption that the target is uniformly distributed within 0.5, 1.0 and 1.5 half-power beamwidths, respectively. The SNR is measured at the center of the sum beam. We see that the proposed detector performs best among the tested detectors in all the three cases. The Classical detector performs well when the target is distributed near the beam center, while the Power-Mosca detector performs good when the target is distributed in a wider range. From Fig. 9 we can deduce that to attain a predefined average probability of detection over the search angular region, the scanning interval can be larger if the dual-stage detector is applied.

Compared to the Classical detector, the increased computational complexity of the dual-stage detector lies in the weight calculation step and the secondary detection step. As the two steps are implemented only when the primary detection is passed, the increased computational complexity is determined by the number of bins that have passed the primary detection, which in the statistical sense is determined by the primary probability of false alarm P_{FA1}. Table 2 shows the comparison

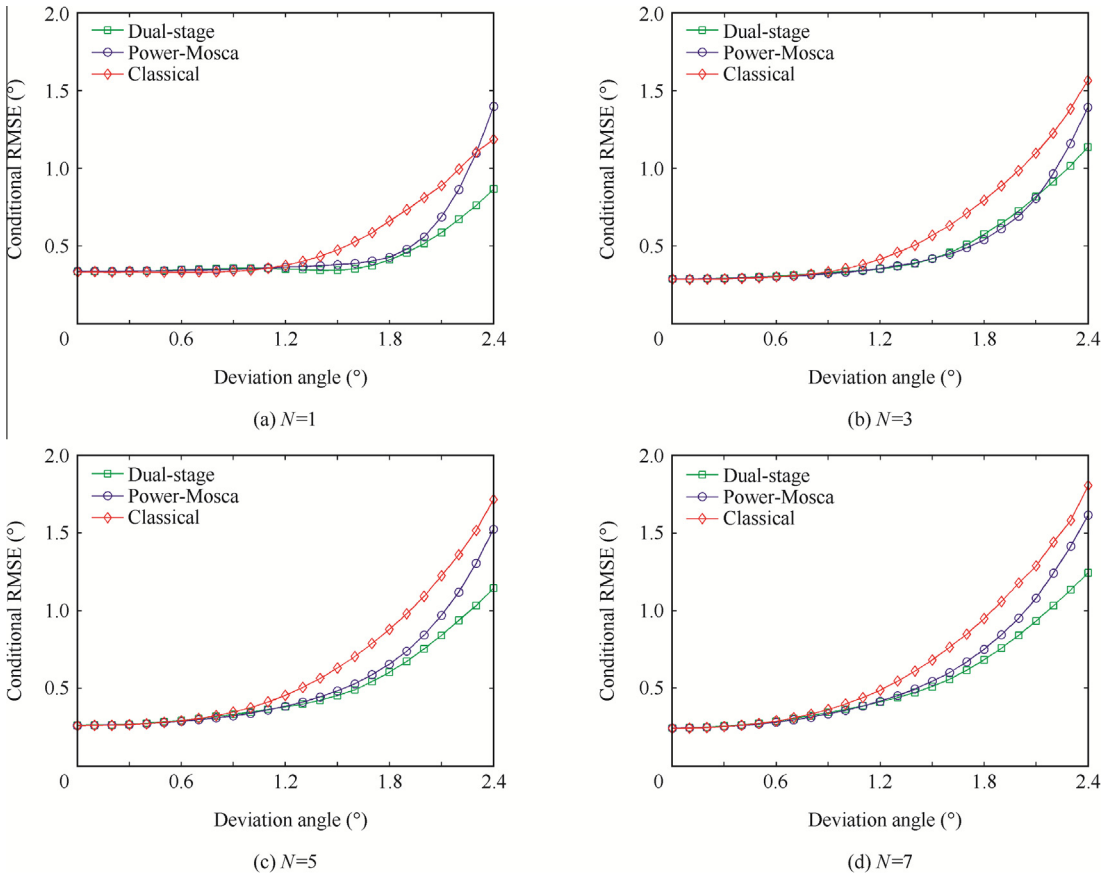

Fig. 8 Conditional RMSE of deviation angle estimation.

of the computational complexity between the three detectors, where K is the number of bins under test, K' is the number of bins that have passed the primary detection, and the operation refers to $+$, $-$, $\times$, $/$ and $\gtrless$ on two real numbers. We see that the computational burden of the Power-Mosca detector is twice that of the Classical detector. Generally speaking, $K' \ll K/2$ because $P_{\mathrm{FA1}} \ll 0.5$. So the computational burden of the proposed dual-stage detector is less than that of the Power-Mosca detector. Table 2 also shows the comparson of the execution time between the three detectors averaged by 10^4 Monte Carlo runs. The three detectors are evaluated in the MATLAB2009a/Slackware14.1 environment on a 3.2 GHz Intel I5 computer with 4 GB of RAM. The number of bins under test is $K = 256$. The pulse number is set as $N = 5$ and thus $P_{\mathrm{FA1}} = 0.05$ is selected. We see that execution time of the dual-stage detector is much lesser than that of the Power-Mosca as expected. Additionally, the estimated $\hat{\gamma}$ can be used directly in the deviation angle estimation once the final detection is declared.

Most radars estimate the direction of arrival in two angular dimensions: azimuth (denoted as y) and elevation (denoted as z). In such systems two difference beams Δ_y and Δ_z are available at the same time. To apply the dual-stage detector to this application, we just need to calculate $\hat{\gamma}_z$ as well as $\hat{\gamma}_y$, and then do secondary stage detection as follows:

$$||\boldsymbol{x}||^2 + ||\hat{\gamma}_y \cdot \boldsymbol{y}||^2 + ||\hat{\gamma}_z \cdot \boldsymbol{z}||^2 > T_2 \tag{21}$$

where $\boldsymbol{z}$ is the signal of Δ_z. Results of the Classical and the dual-stage detectors are shown in Fig. 10. Because of the symmetry between Δ_y and Δ_z, only one Cartesian quadrant is presented. It can be seen that the dual-stage detector outperforms the Classical detector except for performing slightly worse at the beam center.

We have assumed that the target is non-fluctuating from pulse to pulse in the signal model. To see the performance of the dual-stage detector for fluctuating target, Fig. 11 presents the results for Rayleigh fluctuating target. The signal amplitude $|a_i|$ of each pulse is characterized by the randomized distribution:

$$p(|a_i|) = \frac{|a_i|}{\sigma_{\mathrm{a}}^2} \exp\left\{-\frac{1}{2\sigma_{\mathrm{a}}^2}|a_i|^2\right\} \tag{22}$$

where σ_{a} is set to be 1. We can see that the relationship between the performances of the three detectors is similar to the case in the non-fluctuating target.

Remark: Typical tracking radars have a pencil beam and usually depend upon information from outside sensors to acquire the target. But scanning of the beam within a limited angle sector may also be needed to acquire the target within its beam. The angular scanning is generally performed by discrete move of the beam in several angular directions. And the discrete angular interval is limited by the half-power beamwidth. Through increasing the half-power beamwidth equivalently, the dual-stage detector

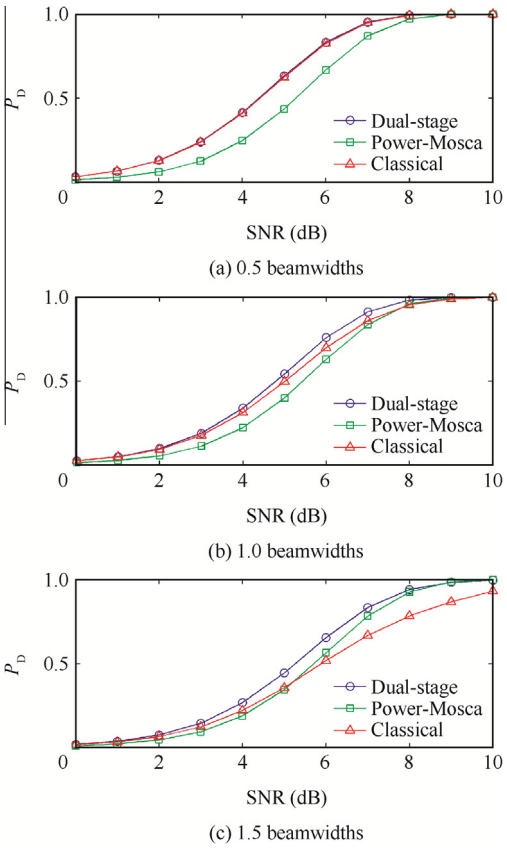

Fig. 9 P_D against SNR for dual-stage detector with target uniformly distributed within certain beamwidths, 5 pulses.

Table 2 Computational complexity.

Detector	Classical	Power-Mosca	Dual-stage
Operation number	$4NK$	$8NK$	$4NK + (8N + 3)K'$
Execution time (ms)	0.413	0.634	0.465

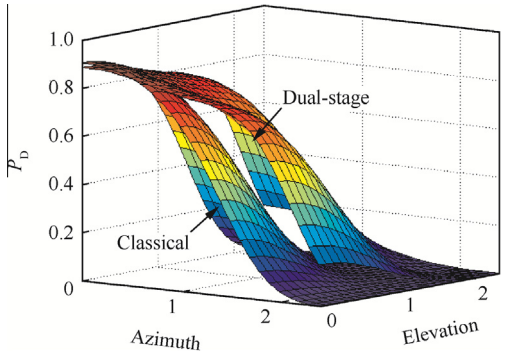

Fig. 10 P_D for dual-stage detector in two angular dimensions, 5 pulses.

can improve the scanning efficiency. The dual-stage detector is also applicable to multi-targets scenario, only if they are located in different range/Doppler resolution bins.

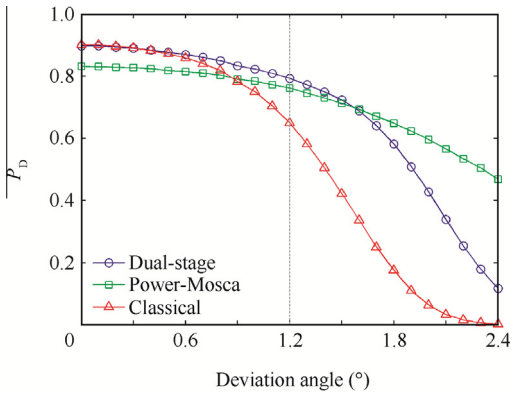

Fig. 11 P_D for fluctuating target, 5 pulses.

6. Conclusions

(1) Two difference beam aided target detectors are proposed. The first one of them is a GLRT detector assuming the monopulse ratio is known. It can be applied when targeting information on target direction is available. After that, a practical dual-stage detector is developed.

(2) Simulation results show that the performance of the dual-stage detector is superior to that of the Classical detector, especially when the deviation angle is nearby the half-power point. As a result, the half-power beamwidth is increased equivalently in the detection performance sense, which is closely related to the scanning speed. Besides, the computational complexity of the dual-stage detector is low and it can be used to replace the Classical detector widely used nowadays.

Acknowledgement

This study was supported by the National Natural Science Foundation of China (Nos. 61101186 and 61401475).

References

1. Skolnik MI. *Radar handbook*. 3rd ed. New York: McGraw-Hill; 2008. p. 417–20.
2. Nickel U. Overview of generalized monopulse estimation. *IEEE Aerosp Electron Syst Mag Part 2: Tutorials* 2006;**21**(6):27–56.
3. Chaumette E, Larzabal P. Monopulse-radar tracking of Swerling III–IV targets using multiple observations. *IEEE Trans Aerosp Electron Syst* 2008;**44**(2):520–37.
4. Chaumette E, Larzabal P. Statistical prediction of monopulse angle measurement. *IET Radar Sonar Navigation* 2007;**1**(5): 377–87.
5. Sherman S. *Monopulse principles and techniques*. Norwood (MA): Artech House; 1984.
6. Kanter I. The probability density function of the monopulse ratio for n looks at a combination of constant and Rayleigh targets. *IEEE Trans Inf Theory* 1977;**23**(5):643–8.
7. Blair W, Brandt-Pearce M. Statistical description of monopulse parameters for tracking rayleigh targets. *IEEE Trans Aerosp Electron Syst* 1998;**34**(2):597–611.
8. Mosca E. Angle estimation in amplitude comparison monopulse systems. *IEEE Trans Aerosp Electron Syst* 1969;**AES-5**(2):205–12.

9. Seifer AD. Monopulse-radar angle tracking in noise or noise jamming. *IEEE Trans Aerosp Electron Syst* 1992;**28**(3):622–37.
10. Seifer AD. Monopulse-radar angle measurement in noise. *IEEE Trans Aerosp Electron Syst* 1994;**30**(3):950–7.
11. Groves G, Blair W, Chow W. Probability distribution of complex monopulse ratio with arbitrary correlation between channels. *IEEE Trans Aerosp Electron Syst* 1997;**33**(4):1345–50.
12. Willet PK, Blair WD, Bar-Shalom Y. Correlation between horizontal and vertical monopulse measurements. *IEEE Trans Aerosp Electron Syst* 2003;**39**(2):533–48.
13. Armstrong B, Griffiths H. Use of difference channel information for detection in monopulse radars. *IEE Proc F* 1991;**138**(3):199–210.
14. Chaumette E, Larzabal P. *Optimal detection theory applied to monopulse antenna. International conference on acoustics, speech, signal processing, 2004 May 17–21*. Piscataway, NJ: IEEE Press; 2004. p. 1065–8.
15. Galy J, Chaumette E, Larzabal P. Joint detection estimation problem of monopulse angle measurement. *IEEE Trans Aerosp Electron Syst* 2010;**46**(1):397–413.
16. Kay SM. *Fundamentals of statistical signal processing: Detection theory*. Englewood Cliffs, NJ: Prentice-Hall; 1998. p. 197–200.
17. Greco M, Gini F, Farina A. Joint use of sum and delta channels for multiple radar target doa estimation. *IEEE Trans Aerosp Electron Syst* 2007;**43**(3):1146–54.
18. Fan HQ. Technology on maneuvering target motion mode identification in active homing guidance dissertation. Changsha: National University of Defense Technology; 2008 [Chinese].
19. Hughes EJ. Radar cross section modeling using genetic algorithms dissertation. Shrivenham: Royal Military College of Science; 1998.
20. Chaumette E, Larzabal P, Forster P. On the influence of a detection step on lower bounds for deterministic parameter estimation. *IEEE Trans Signal Process* 2005;**53**(11):4080–90.

Cai Fei received B.S. and M.S. degrees from the National University of Defense Technology (NUDT) in 2008 and 2011 respectively. Currently he is pursuing the Ph.D. degree in the ATR Key Laboratory, NUDT. His area of research includes radar signal and data processing, target detection and tracking.

Fan Hongqi received the B.S. degree in mechanical engineering and automation from Tsinghua University in 2001, and the Ph.D. degree in information and communication engineering from NUDT in 2008. He is currently an associate professor at NUDT. His research interests include radar signal processing, target tracking and information fusion.